



Impact of binaries on stellar evolution in the Gaia era

A. Jorissen

Institut d'Astronomie et d'Astrophysique, Université Libre de Bruxelles C.P. 226, Avenue F. Roosevelt 50, B-1050 Bruxelles, Belgium, e-mail: ajorisse@ulb.ac.be

Abstract. This paper first reviews specific classes of stars which are the outcome of binary evolution, putting emphasis on some recent results, not necessarily related to *Gaia* research: Algols, blue stragglers, barium stars and related families (barium dwarfs and giants, carbon dwarfs, subgiant CH and giant CH, CEMP-s, S stars without Tc), post-RGB stars, sdB stars, and (asymmetric) planetary nebulae. We then describe some of the assets that *Gaia* data offer to the binary-star researcher, stressing as well the pitfalls awaiting on the road, using as a specific example the placement of barium stars in the Hertzsprung-Russell diagram. In particular, we evaluate the usefulness of the *Gaia* DR2 RUWE ('renormalised unit-weight error') parameter in the context of identifying astrometric binaries.

Key words. binaries: general – blue stragglers – Stars: peculiar – Astrometry – Stars: evolution

1. Introduction

Starting from the solution of the Algol paradox in terms of a specific stage in the evolution of binary systems with mass-ratio reversal due to strong mass exchange (see Paczyński 1971, and references therein), the impact of binaries on stellar evolution has since been an ever-growing field with many surprises. Another among the early-identified major impacts of duplicity on stellar evolution is the creation of blue stragglers in the final stage of an Algol-like binary evolution (McCrea 1964; Paczyński 1971; Webbink 1985). Since these major findings, binary systems have been identified to impact stellar evolution in several other circumstances, those being reviewed here all deal with binary systems involving low- and intermediate-mass stars. For massive systems, we refer to Sana et al. (2012) and references therein. Very extensive reviews on the

same topic, covering the full stellar mass range, may be found in Eggleton (2011), De Marco & Izzard (2017), and Beccari & Boffin (2019).

In Sect. 2, we briefly review specific classes of stars which are the outcome of binary evolution, putting emphasis on some recent results, not necessarily related to *Gaia* research. In Sect. 3, we describe some of the assets that *Gaia* data offer to the binary-star researcher, stressing as well the pitfalls awaiting on the road, using as an example the study of Escorza et al. (2017, 2019a,b) locating barium stars in the Hertzsprung-Russell diagram (HRD).

2. Classes of stars requiring duplicity

2.1. Algols

A binary is considered an Algol when the semi-detached system shows the typical characteris-

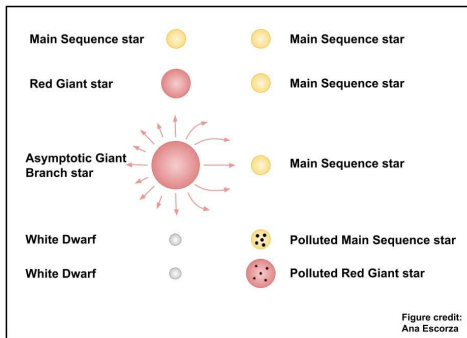


Fig. 1. A schematic view of the mass-transfer scenario responsible for the formation of barium stars, labelled ‘Polluted Main Sequence star’ and ‘Polluted Red Giant star’ in the figure.

tics as mentioned by Peters (2001), i.e., the less massive donor fills its Roche lobe, the more massive gainer does not fill its Roche lobe and is still on the main sequence (usually of spectral types B-A) and the donor is the cooler, fainter and larger star (usually a cool F-K giant star). Their orbital periods are usually short (from several hours to tens of days; Giuricin et al. 1983). Despite the fact that mass transfer occurs via Roche-lobe overflow (RLOF), which is generally considered to be conservative (i.e., with no mass lost from the system), it has been shown that the RLOF leading to Algol systems must be non-conservative (with angular momentum being lost by the system) to comply with observations of mass ratios (e.g., Refsdal et al. 1974; Masevitch & Yungelson 1975; Sarna 1993; van Rensbergen et al. 2006, 2011). However, the exact mechanism driving this systemic mass loss is still under debate (see e.g., Deschamps et al. 2013, 2015, and references therein). Nonetheless, Deschamps et al. (2015) and Mayer et al. (2016) present observational signatures clearly demonstrating that the mass transfer is non-conservative, leaving behind extended circumstellar envelopes which have been imaged with the Wide-field Infrared Survey Explorer (WISE) satellite (Wright et al. 2010) and which even show interaction with the circumstellar medium in the form of bow shocks.

2.2. Blue stragglers

Among the early-identified major impacts of duplicity on stellar evolution is the recognition that blue stragglers (McCrea 1964) result from an Algol-like binary evolution (Paczynski 1971; Webbink 1985). The recent developments in that field involve the search for chemical signatures of pollution, in the form of enhanced carbon or heavy elements produced by the s-process of nucleosynthesis (Käppeler et al. 2011), as in barium and related stars (Sect. 2.3). The pollution was caused by mass transfer originating from a low- or intermediate-mass star at the asymptotic giant branch (AGB) stage of its evolution, in a similar way as that causing the barium-star syndrome (e.g., Boffin & Jorissen 1988; Mohamed & Podsiadlowski 2012, and Fig. 1). The association of blue stragglers with such a mass-transfer episode was first proposed by Preston & Sneden (2000) for field blue metal-poor (BMP) stars. However, despite the larger than usual binary frequency observed among those BMP stars, in favour of their blue-straggler mass-transfer origin, no clear barium-star case was found. The more recent study of blue stragglers in the open cluster NGC 6819 by Milliman et al. (2015) was more successful in that respect, as several barium stars were indeed found among them. However, the situation regarding binarity is confusing: blue-straggler barium stars do not show evidence of binarity and conversely. The reason for this deviation from the usual mass-transfer paradigm is unclear so far. The old open cluster NGC 188 has been shown to contain blue stragglers with WD companions (Gosnell et al. 2014, 2015; Subramaniam et al. 2016), which are ideal targets to clarify the conditions of occurrence of the barium syndrome (on that issue, see also Merle et al. 2014; Jorissen et al. 2019). Incidentally, Gosnell et al. (2015) provide orbital elements for 16 NGC 188 blue stragglers, whose location in the eccentricity – period diagram is strikingly similar to that of the post-AGB systems (panels (h) and (i) in Fig. 2 and Oomen et al. 2018), thus confirming the mass-transfer origin of the blue stragglers.

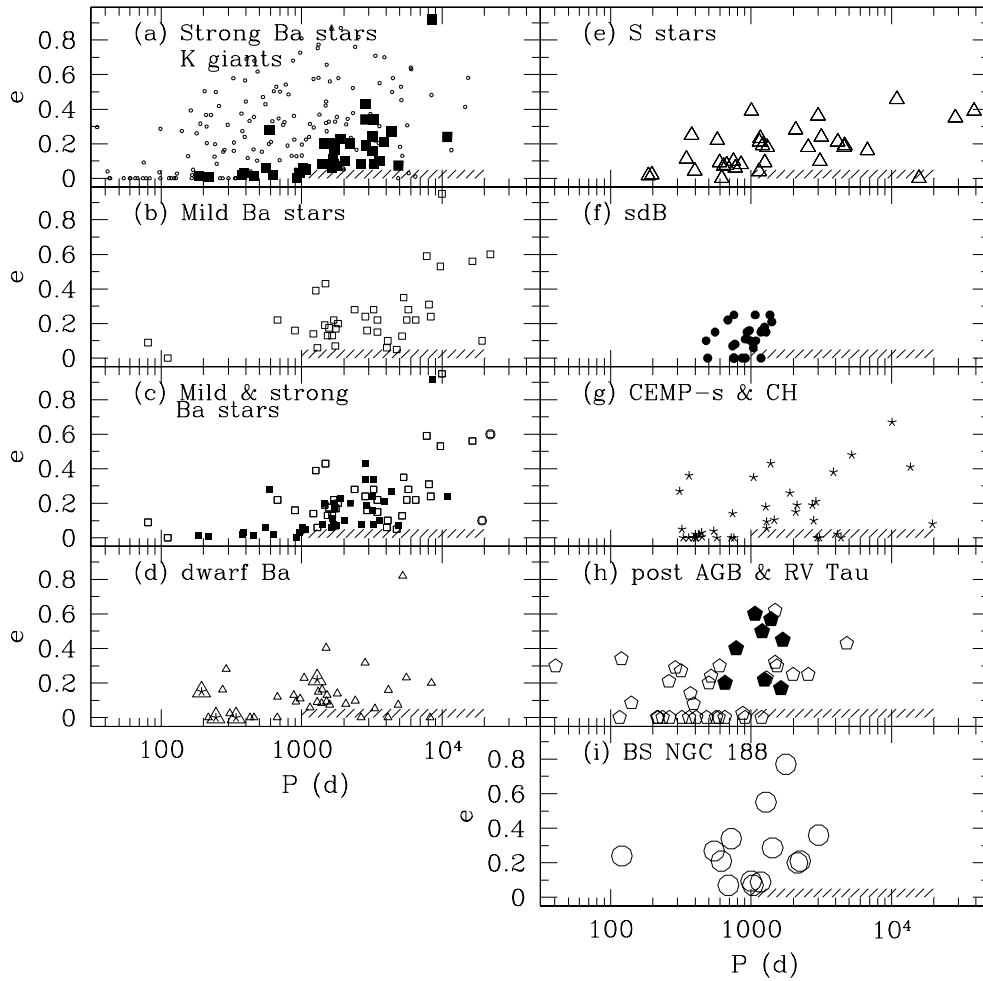


Fig. 2. A compendium of eccentricity – period diagrams for post-mass-transfer binaries: **(a)** Strong barium stars (large filled squares; with orbital data from Van der Swaelmen et al. 2017 and Jorissen et al. 2019), along with the comparison sample of (mostly) pre-mass-transfer binaries (G and K giants in open clusters from Mermilliod et al. 2007, small open circles). The lower-right hatched area corresponds to an avoidance zone (see e.g., Jorissen et al. 2019, for a discussion); **(b)** Mild barium stars, small open squares, with data as for (a); **(c)** Strong and mild barium stars altogether; **(d)** dwarf and subgiant barium and CH stars, with data from McClure (1997) and Escorza et al. (2019a) (open triangles), and a few dwarf CEMP-s stars (crossed open triangles) from Sneden et al. (2003) and Dearborn et al. (1986). Systems falling in the avoidance region likely have inaccurate orbits. Some dwarf CEMP-s and carbon stars, not represented on the figure, may have orbital periods as short as a few days (Green et al. 2019, and references therein); **(e)** S stars (open triangles), with data as for (a); **(f)** sdB binaries (filled circles), with data from Deca et al. (2012), Vos et al. (2012), Barlow et al. (2012), and Vos et al. (2019); **(g)** CH, CH-like, and CEMP-s stars (crosses), with data from McClure & Woodsworth (1990), Sperauskas et al. (2016), Hansen et al. (2016), and Jorissen et al. (2016); **(h)** post-AGB (open pentagons) and RV Tau (filled pentagons), with data from Oomen et al. (2018) and Manick et al. (2019); **(i)** NGC 188 blue stragglers (large open circles), with data from Gosnell et al. (2015). There are two more binaries with periods around 5 d, which are not displayed.

2.3. Barium stars and related families

Barium stars and their relatives (barium dwarfs, carbon dwarfs¹, subgiant CH and giant CH, CEMP-s, S stars without Tc) are the prototypical examples of post-mass-transfer binaries, where mass transfer left its chemical imprint in the form of excess carbon and s-process elements. A dynamical signature exists as well in the form of a flatter eccentricity – period diagram, and this effect may be readily identified by comparing barium stars with normal K giants in panel (a) of Fig. 2 (see also Fig. 1 of Escorza et al. 2019b).

Thanks to a very long-lasting radial-velocity monitoring (Jorissen et al. 2019; Escorza et al. 2019a), the upper limit of the period distributions has now been reached for giant barium stars with strong chemical anomalies (the so-called ‘strong barium stars’) and S stars, and it amounts to about $1 - 3 \times 10^5$ d, or 30 – 100 yr. This first-hand collection of 132 post-mass-transfer systems with available orbital elements (105 giant and 27 dwarf and subgiant barium stars) has been used to derive the mass distributions of barium stars (see Sect. 3) and of their white-dwarf (WD) companions (Jorissen et al. 2019; Escorza et al. 2019b). The latter spans the range $0.55 - 0.85 M_{\odot}$, as expected for CO WDs, with a few more massive candidates (up to $1 M_{\odot}$), the latter thus pointing towards initial AGB masses below $5 M_{\odot}$, just compatible with current expectations for AGB s-process nucleosynthesis (Cristallo et al. 2015; Karakas & Lugaro 2016).

2.4. Leaving the red-giant branch prematurely: Post-RGB, sdB and He WD stars

Mass transfer from a red-giant branch (RGB) donor star, and the subsequent premature end of the evolution of that RGB star, lead to stellar families specifically requiring binary interaction like subdwarf B (sdB) stars (e.g., Vos et

al. 2019) and He WDs (e.g., Merle et al. 2014; Siess et al. 2014). Subdwarf B stars are core-helium-burning stars with a very thin hydrogen envelope ($M_{\text{H}} < 0.02 M_{\odot}$), and a mass close to the core-helium-flash mass ($\sim 0.47 M_{\odot}$; Heber 2016).

This evolutionary path differs from that leading to Algols sketched in Sect. 2.1 in that the mass donor is now a RGB star with a deep convective envelope. In such circumstances, when the mass ratio (donor/gainer) is larger than some critical value $q_c < 1$ (see Chen & Han 2008, for details), as it is initially, RLOF mass transfer is dynamically unstable and may lead to common-envelope evolution, leading to dramatic orbital shrinkage and even coalescence (Webbink 1984). Since many sdB stars with long orbital periods (in the range 500 – 1500 d) are now known (see Vos et al. 2019, and panel (f) in Fig. 2), they must result instead from stable RLOF, which implies that the mass ratio must be smaller than $q_c (< 1)$ at the onset of RLOF (Chen & Han 2008). The situation is even more complex when the post-mass-transfer eccentricity turns out to be non-zero, since RLOF is known to circularise the orbits. Nevertheless, non-zero eccentricities are often encountered among sdB binaries (see panel (f) in Fig. 2). An evolutionary path matching these constraints was found by Siess et al. (2014), in the specific case of the K0 IV + He-WD system IP Eri (Merle et al. 2014), with $P = 1071$ d and $e = 0.25$. The only solution to form a He WD and preserve some eccentricity in a long-period system is to remove mass from the giant while keeping it well inside its Roche radius so that the circularising tidal effects remain weak. One possibility to meet these requirements is to boost the wind mass-loss rate on the RGB as proposed by Tout & Eggleton (1988) through the so-called ‘Companion-reinforced attrition process’ (CRAP). Siess et al. (2014) solution requires as well that the initial mass ratio of the system be just above unity (namely 1.5 + $1.45 M_{\odot}$ in the case of IP Eri).

A new member has recently been added to the family of binary systems leaving the RGB, with the discovery by Kamath et al. (2014, 2015, 2016) in the Magellanic Clouds of the so-called ‘post-RGB stars’, by analogy

¹ Although very few orbital elements are available for dwarf carbon stars, there is ample evidence that they host a very large fraction of binaries, as shown by e.g., Whitehouse et al. (2018) and Roulston et al. (2019).

to the well-known ‘post-AGB stars’ (see Van Winckel 2003, for a review). As for their post-AGB analogs, the binary post-RGB stars are enshrouded in a dusty disc. *Gaia* now offers the possibility to find such systems in our Galaxy.

2.5. Axisymmetric planetary nebulae

Planetary nebulae (PNe) were traditionally considered to represent the final evolutionary stage of all stars in the mass range ~ 0.7 to $8 M_{\odot}$. Recent evidence seems however to contradict this picture. In particular, it has become clear that PNe display a wide range of striking morphologies which cannot be understood in the framework of a single-star scenario, pointing instead towards a binary evolution in a majority of systems. A good summary of our current understanding of the importance of binarity in the formation and shaping of PNe is presented by Jones & Boffin (2017), and references therein. Major advances in that field are the following. First, many PNe (especially axisymmetric ones) actually seem to be the outcome of common-envelope evolution (Webbink 1984), with the central stars of those PNe (CSPN) being short-period binaries (with periods ranging from a few hours to a few days). However, PNe do not only harbour short-period binaries, since an increasing number of PNe are now found to host long-period binaries as well (Van Winckel et al. 2014; Jones et al. 2017), which cannot be the result of common envelope evolution. Second, several (binary) CSPN exhibit chemical signatures of mass transfer, in the form of enhanced carbon (like for the central star of PN G054.2-03.4 – ‘The Necklace’ – which reveals a dC spectrum; Miszalski et al. 2013b) and/or s-process elements (Bond et al. 2003; Miszalski et al. 2012, 2013a), similar to the barium stars described in Sect. 2.3. These PNe tend to present an apparent ring-like morphology, which is most likely the outcome of the mass-transfer episode – probably by wind – that led to the pollution of the cool secondary star in carbon and s-process elements. At least some of these, like HD 112313 (CSPN in LoTr5), are indeed both long-period binaries and enriched in s-process elements (Van Winckel et al. 2014; Thevenin

& Jasniewicz 1997), as required by the barium-star paradigm described above. But on the contrary, the KIII component of the central binary in LoTr1, despite showing a rapid rotation signalling that it is harboured by a post-mass-transfer system, does not show s-process enrichment. This illustrates once more that some other conditions need to be met to produce a barium star in a binary system (Tyndall et al. 2013; Merle et al. 2016; Jorissen et al. 2019).

3. In the Gaia era: assets and pitfalls

Gaia will offer many assets to the binary-star researcher, but there are as well pitfalls along the road, and we review both in this section, using as an example the study of Escorza et al. (2017, 2019a,b) locating barium stars in the Hertzsprung-Russell diagram (HRD).

3.1. Location in the Hertzsprung-Russell diagram

The specific problems arising when trying to locate stars in the HRD were reviewed by Babusiaux (*Gaia* Collaboration et al. 2018), so that we provide here just a basic summary. First, if the goal is to derive masses, the stars have to be located in a (T_{eff} , $\log L/L_{\odot}$) diagram (as opposed to a colour – absolute-magnitude diagram) in order to compare their location with evolutionary tracks computed from stellar-evolution codes. The effective temperature must then be derived from usual spectroscopic or photometric methods. As an example of the latter, Escorza et al. (2017) matched observed spectral energy distributions (SEDs) with reddened synthetic SEDs (obtained from MARCS models; Gustafsson et al. 2008), knowing that there is a strong correlation between reddening E_{B-V} and T_{eff} . Therefore, it was necessary to either fix T_{eff} to its value obtained from spectroscopy (as in Fig. 3), or as in Escorza et al. (2017), to constrain E_{B-V} by the extinction map of Gontcharov (2012). The extinction is part of *Gaia* DR2, but as Fig. 3 reveals, *Gaia* DR2 A_G values are significantly different from those obtained by fitting the SED with T_{eff} fixed at its spectroscopic value.

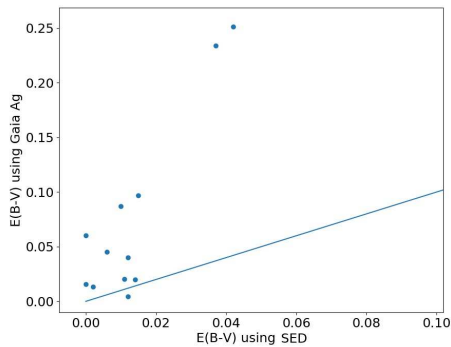


Fig. 3. Comparison of the reddening obtained from *Gaia* DR2 and from SED fitting with T_{eff} fixed from spectroscopy, for those dwarf barium stars from Table 3 of Escorza et al. (2019a) with A_G available in *Gaia* DR2.

Luminosity may be derived by combining any apparent magnitude and the corresponding bolometric correction (derived by integrating the best-matching synthetic SED) with the distance modulus. The distance may be derived by inverting the parallax if its relative error does not exceed 10%; if it does, Bayesian distance estimates must be used instead (e.g., Bailer-Jones et al. 2018) to avoid the biases in the distances that would result from a simple parallax inversion (Bailer-Jones 2015; Luri et al. 2018).

3.2. Binary-star parallaxes

The DR2 parallaxes were derived with a single-star (5-parameter astrometric) model (as will be the early DR3 parallaxes), thus not allowing for any binary motion. What are the consequences of this inconsistency on the parallax accuracy for binary systems? How trustworthy are the *Gaia* DR2 parallaxes for the purpose of deriving the luminosity of the primary-star component in a binary system? In the remainder of this section, we will demonstrate that the answer to this question is fortunately positive: except in a few cases (mostly concentrated around orbital periods close to 1 yr), the *Gaia* DR2 parallaxes derived for binary systems with a single-star model are correct to within 10 to 20%.

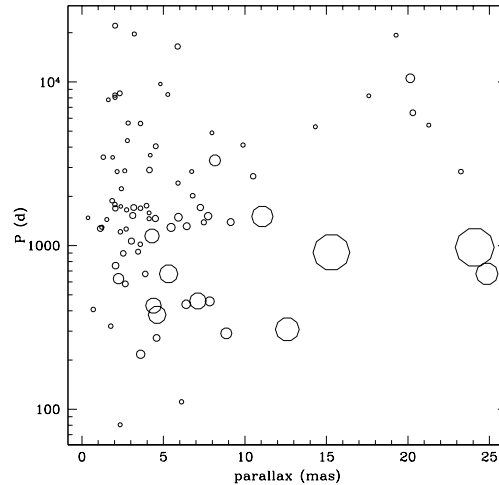


Fig. 4. The RUWE parameter is proportional to the symbol size in this DR2 parallax – orbital period plane, for the barium stars studied by Van der Swaelmen et al. (2017), Escorza et al. (2017, 2019a,b), and Jorissen et al. (2019), all of them being spectroscopic binaries. The largest circle corresponds to HD 34654 with $\text{RUWE} = 9.5$.

Gaia DR2 contains several statistical indicators that can be used to assess the quality and reliability of the astrometric solution. One such indicator is the astrometric chi-square, or equivalently the unit weight error (UWE), which is the square root of the reduced chi-square. The usefulness of the UWE parameter is however severely hampered by its strong sensitivity to magnitude and colour. This sensitivity can be eliminated by a re-normalisation process, using tables providing average UWE values across the colour – magnitude plane (Lindgren 2018). The re-normalised UWE (or RUWE) is a more reliable and informative goodness-of-fit statistic which allows to evaluate the quality of the astrometric solution better than for example the astrometric excess noise or astrometric chi-square. This recent addition to *Gaia* DR2 is available as a separate table next to the main *Gaia* DR2 table, both being easily accessible through the TOPCAT utility (<http://www.starlink.ac.uk/topcat>) and its Table Access Protocol (TAP) query (select *Gaia* DR2). RUWE values smaller than about

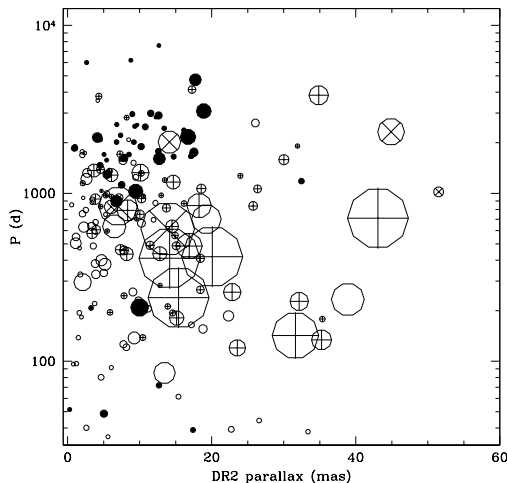


Fig. 5. Same as Fig. 4 for the spectroscopic binaries from the SB9 catalogue. The largest circles correspond to $\text{RUWE} > 15$. The circled plus (\oplus) symbols correspond to DMSA/O entries (i.e., HIPPARCOS orbital astrometric binaries) in the Double and Multiple Star Annex of the Hipparcos Catalogue (ESA 1997), the circled cross (\otimes) to DMSA/X (i.e., stochastic) solutions, and the filled circles to DMSA/G (i.e., acceleration) solutions.

1.4 flag good astrometric solutions (Lindgren 2018).

Figure 4 shows the RUWE values in the parallax – orbital period plane, for the barium stars studied by Van der Swaelmen et al. (2017), Escorza et al. (2017, 2019a,b), and Jorissen et al. (2019). It is very clear that the RUWE parameter is a good indicator of binarity in *Gaia* DR2, at least for parallaxes in excess of a few mas and for orbital periods shorter than about 1500 d. Given the known sensitivity of *Gaia* data to the brightness (and colours) of the targets (see e.g., Lindgren 2018), we stress however that this statement is based on the analysis of binary systems whose primary component has a visual magnitude in the range ~ 6 to ~ 10 , and cannot at this stage be safely extrapolated outside this range (see also the discussion by Pourbaix 2019).

A similar plot for the larger sample of binary stars extracted from *The ninth catalogue of spectroscopic binary orbits* (SB9; Pourbaix et al. 2004) has been presented in

Fig. 5. Clearly, for this large sample as well, the largest RUWE values correspond to binary systems which fall in the region where the astrometric binary motion is best detectable by the *Gaia* DR2 data (namely, with parallax $\varpi_{\text{DR2}} \gtrsim 10$ mas and $P \lesssim 1000$ d). Since the time span of *Gaia* DR2 (668 d) is similar to that of Hipparcos (about 1000 d; ESA 1997), it is possible to compare *Gaia* DR2 RUWE diagnostic with those provided by the Double and Multiple Star Annex (DMSA) of the Hipparcos Catalogue in terms of astrometric orbit (DMSA/O), accelerated proper motion (DMSA/G) or stochastic solution (DMSA/X). This is performed on Fig. 5, which clearly shows that basically all stars with large RUWE values were flagged as well by Hipparcos as either DMSA/O or DMSA/X. There is thus no reason to believe that some extra noise source contaminates the RUWE value apart from the binary motion. The DR2 RUWE parameter may not however serve as an efficient diagnostic to unravel binary systems, since for orbital periods larger than about ~ 1000 d, the orbital motion causes accelerated proper-motion solutions (DMSA/G in Hipparcos; filled circles in Fig. 5), and the RUWE parameter loses most of its efficiency in detecting those binary systems. The situation is similar at small parallaxes or short orbital periods. Incidentally, Fig. 6 shows another possible diagnostic to flag binary stars, advocated by D. Boubert² (although in a more sophisticated version, including an estimate of the instrumental error) and based on the ‘radial-velocity error’ (actually standard deviation rather than ‘error’) as provided by *Gaia* DR2. Although that diagnostic offers a good detection efficiency for systems with orbital periods up to 1000 d (Fig. 6), its efficiency obviously decreases as well at longer periods.

Coming back to the RUWE parameter, by definition, large RUWE values indicate that the astrometric single-star solution is inadequate. But does this necessarily mean that the parallax is inaccurate? As we now show, the answer to

² https://www.arcetri.inaf.it/~mathieu/.EwAsS-2019-SS22/301_ss22a_0950_boubert.pdf

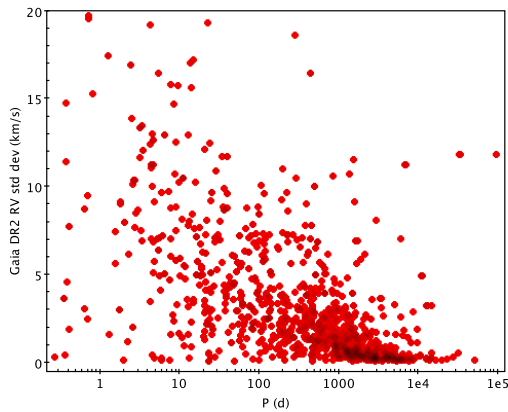


Fig. 6. The standard deviation of *Gaia* DR2 radial velocities (listed as ‘radial-velocity error’ in *Gaia* DR2) as a function of the orbital period for the full sample of SB9 systems.

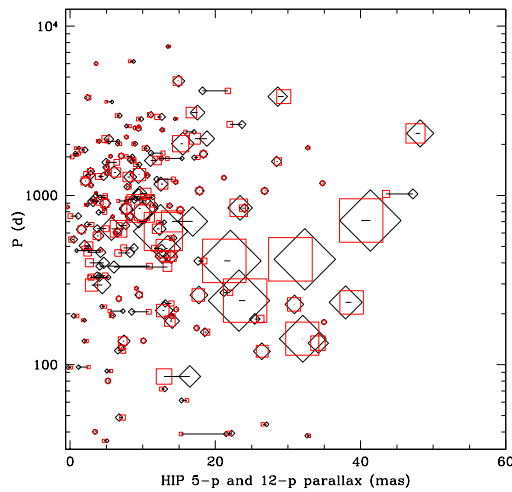


Fig. 7. Comparison of the parallaxes obtained with single-star (5-parameter) and acceptable binary-star (12-parameter) solutions (tilted squares and horizontal red squares, respectively) for the spectroscopic binaries from the SB9 catalogue (from Jancart et al. 2005, reprocessing the *Hipparcos Intermediate Astrometric Data*). The symbol size is proportional to the *Gaia* DR2 RUWE parameter, as in Figs. 4 and 5.

that question is in fact negative in most cases. To investigate this question, data from Jancart et al. (2005) may be used. These authors have reprocessed the *Hipparcos Intermediate*

Table 1. Parallaxes for systems with orbital periods closest to 1 yr among those reprocessed by Jancart et al. (2005). Columns labelled ϖ_{5-p} and ϖ_{12-p} designate Hipparcos parallaxes obtained with a single-star (‘5-parameter’) model and a binary-star (‘12-parameter’) model (not published in the original paper).

HIP	P (d)	ϖ_{5-p} (HIP) (mas)	ϖ_{12-p} (mas)	RUWE DR2
2865	399.6	4.6 ± 0.8	2.7 ± 2.4	2.8
26291	381.7	4.1 ± 0.9	10.9 ± 5.8	2.0
100738	377.6	6.0 ± 0.9	13.4 ± 12.1	3.0

Astrometric Data (IAD) with a binary solution (along the guidelines discussed by Pourbaix & Jorissen 2000, but with a more efficient statistical filtering) for all binary systems listed in the SB9 catalogue at the time, and kept the binary solution if it satisfies several quality checks. For those retained binary solutions (which constitute the sample plotted in Fig. 5), it is then possible to compare the parallaxes obtained with the single-star (‘5-parameter’) and with the binary-star (‘12-parameter’) solutions (data not originally published by Jancart et al. 2005), and see by how much they differ, as shown on Fig. 7. The same data are presented in a slightly different way in Fig. 8. It is clear that the systems with the largest RUWE values are by no means those with the largest shifts between the 5-parameter and 12-parameter parallaxes. Not only are large shifts found for systems with orbital periods close to 1 yr, but the parallax obtained with the binary model is very uncertain (Table 1). This is because the parallactic and orbital signals both vary on a 1 yr time scale, and cannot be disentangled.

Pourbaix (2019) has made a similar comparison between ϖ_{5-p} and ϖ_{12-p} parallaxes, while searching for astrometric binaries in a random sample of 10^5 stars using pre-DR3 (AGIS 3.1) data. The difficulty of finding reliable solutions for systems with periods close to 1 yr is again illustrated by the gap observed on the right panel of Pourbaix’s Fig. 3. A new behaviour, not seen in the re-processing of the *Hipparcos* IAD discussed above, is the rising trend of the $\varpi_{12-p}/\varpi_{5-p}$ ratio at small parallaxes (middle panel of Fig. 3 in Pourbaix

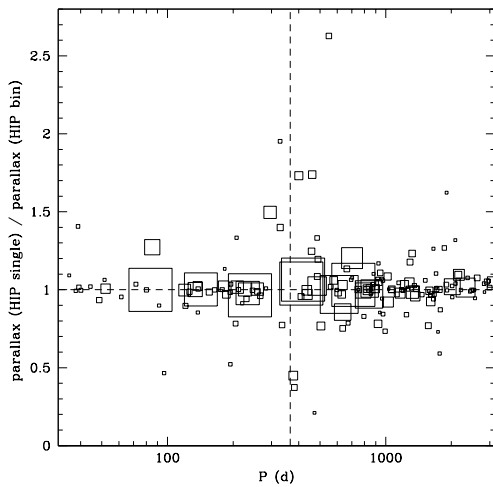


Fig. 8. Same as Fig. 7 but for $\varpi_{5-p}/\varpi_{12-p}$ (Hipparcos) as a function of orbital period P . The vertical dashed line marks $P = 1$ yr.

2019). For reasons unexplained so far, this increase is however limited to the period range 400 – 600 d (see the location of blue triangles in Fig. 9). Figure 9 displays the same data, but in the parallax – period plane, and moreover adds to the pre-DR3 sample the barium stars studied by Escorza et al. (2017, 2019a,b) and Jorissen et al. (2019). This comparison offers a new way to test the reliability of the DR2 parallaxes of barium stars used in the aforementioned studies. Again, it appears clearly that only few barium stars are at risk of having unreliable DR2 parallaxes (as stressed in the original papers, those are CD $-64^{\circ}4333$, HD 24035, and HD 209621 with periods of 386 d, 378 d, and 407 d, respectively). Most of the barium stars actually fall in the region not yet explored by the *Gaia* pre-DR3 data (since the associated time span is only about 800 d). In that region of long orbital periods, the unresolved binary motion would show up as an acceleration solution, as it was shown by Fig. 5, and acceleration- or binary-model parallaxes are not very different from single-star parallaxes, as can be seen by locating the DMSA/G solutions from Fig. 5 (filled circles) in Fig. 7.

To conclude this section, it may thus be asserted that the use of DR2 parallaxes to locate

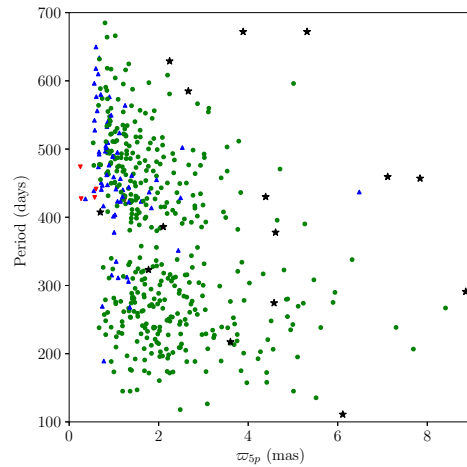


Fig. 9. Properties of the astrometric binaries found in a random sample of 10^5 stars using pre-DR3 (AGIS 3.1) data (see also Fig. 3 of Pourbaix 2019), in the parallax – period plane, with colors and symbols referring to the $\varpi_{12-p}/\varpi_{5-p}$ ratio, as follows: green circles: < 1.5 , blue triangles pointing upwards: $1.5 - 2.0$, red triangles pointing downwards: ≥ 2 . Barium stars studied by Van der Swaelmen et al. (2017), Escorza et al. (2017, 2019a,b), and Jorissen et al. (2019) are represented as black stars.

binary systems in the HRD, as done by Escorza et al. (2017, 2019a,b) and Jorissen et al. (2019), is fully justified, except when the orbital period falls in the range 330 – 400 d for any value of the parallax, or in the range 400 – 600 d for parallaxes smaller than 1 mas.

3.3. Masses

We conclude this review of the pitfalls involved in deriving stellar masses from the location in the HRD by the problems specific to evolutionary tracks. First, their location in the HRD is very sensitive to metallicity (e.g., Fig. 8 of Escorza et al. 2017), so that the stars of interest should have their metallicity known beforehand. It appears for instance that, in the region occupied by the He clump, the $[\text{Fe}/\text{H}] = -0.5$ track of a $2.0 M_{\odot}$ star covers the same region as the $[\text{Fe}/\text{H}] = 0$ track of a $3.0 M_{\odot}$ star, leading to a strong degeneracy in the mass determina-

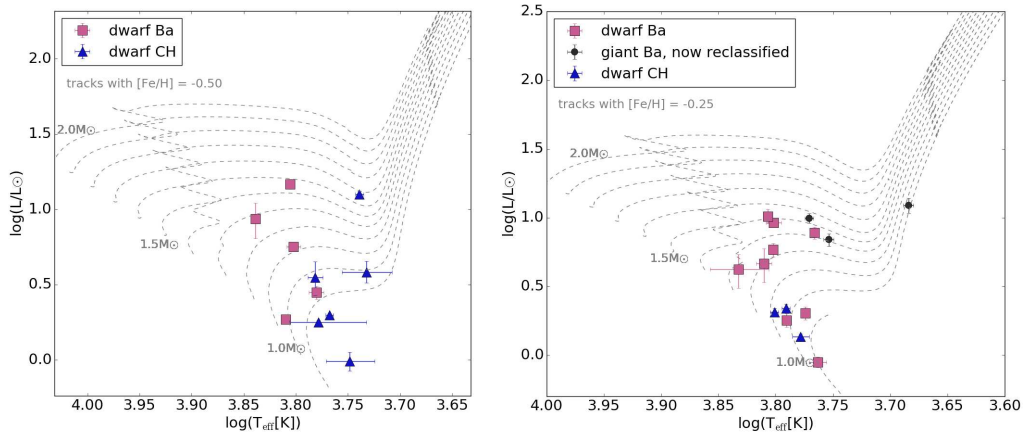


Fig. 10. The various subclasses of barium stars (namely, dwarf Ba stars, dwarf CH stars, CH subgiants, and giant Ba stars; left panel: $[\text{Fe}/\text{H}] = -0.50$, right panel: $[\text{Fe}/\text{H}] = -0.25$) falling in the dwarf and subgiant regions of the HRD (from Escorza et al. 2019a), revealing the need for a spectral re-classification of the members of these families.

tion of a given star, which can only be lifted by knowing its metallicity.

Second, in some regions of the HRD, tracks of different masses and evolutionary stages (with the same metallicity) pass close to each other. In those cases, the choice of the most probable track may be done using arguments based on the evolutionary time spanned in a given neighbourhood of the star of interest, as described by Escorza et al. (2017).

In terms of assets, Fig. 10 shows the location of various members of the subclasses of barium stars (namely, dwarf Ba stars, dwarf CH stars, CH subgiants, and giant Ba stars) falling in the dwarf and subgiant regions of the HRD (from Escorza et al. 2019a), and reveals the need for a spectral re-classification of the members of these families. Indeed, CH subgiants and barium dwarfs are mixed together in the dwarf region of the HRD, and there seems to be no need for calling them differently. Moreover, several barium stars, previously classified among the classical (giant) barium stars, turn out to be closer to subgiants in fact.

Finally, when it comes to the derivation of individual *companion* masses from orbital elements, the above procedure (which yields the mass of the *visible* component of the binary

system) must be complemented by the knowledge of the orbital inclination i . This should await the release of the astrometric orbital elements in *Gaia* DR3, which will render obsolete the various tricks used so far to circumvent the unavailability of i , as described by Escorza et al. (2019a,b) and Jorissen et al. (2019).

Acknowledgements. I thank D. Pourbaix for interesting discussions which led to Fig. 9. I thank A. Escorza for preparing Figs. 1 and 3. This research has been funded by the Belgian Science Policy Office under contract BR/143/A2/STARLAB, and by the Fonds National de la Recherche Scientifique (F.R.S.-FNRS), Belgium. Based on observations obtained with the HERMES spectrograph, which is supported by the Research Foundation – Flanders (FWO), Belgium, the Research Council of KU Leuven, Belgium, the Fonds National de la Recherche Scientifique (F.R.S.-FNRS), Belgium, the Royal Observatory of Belgium, the Observatoire de Genève, Switzerland and the Thüringer Landessternwarte Tautenburg, Germany.

References

- Bailer-Jones, C. A. L. 2015, *PASP*, 127, 994
- Bailer-Jones, C. A. L., Rybizki, J., Fouesneau, M., et al. 2018, *AJ*, 156, 58
- Barlow, B. N., Wade, R. A., Liss, S. E., et al. 2012, *ApJ*, 758, 58

- Beccari, G., & Boffin, H. (eds.), 2019, *The Impact of Binary Stars on Stellar Evolution* (Cambridge University Press, Cambridge)
- Boffin, H. M. J., & Jorissen, A. 1988, *A&A*, 205, 155
- Bond, H. E., Pollacco, D. L. & Webbink, R. F. 2003, *AJ*, 125, 260
- Chen, X., & Han, Z. 2008, *MNRAS*, 387, 1416
- Cristallo, S., Straniero, O., Piersanti, L., et al. 2015, *ApJS*, 219, 40
- Dearborn, D. S. P., Liebert, J., Aaronson, M., et al. 1986, *ApJ*, 300, 314
- Deca, J., Marsh, T. R., Østensen, R. H., et al. 2012, *MNRAS*, 421, 2798
- De Marco, O., & Izzard, R. G. 2017, *Publ. Astron. Soc. Australia*, 34, e001
- Deschamps, R., Siess, L., Davis, P. J., et al. 2013, *A&A*, 557, A40
- Deschamps, R., Braun, K., Jorissen, A., et al. 2015, *A&A*, 577, A55
- Eggleton, P. 2011, *Evolutionary Processes in Binary and Multiple Stars* (Cambridge University Press, Cambridge)
- ESA 1997, *The Hipparcos and Tycho Catalogues*, ESA Special Publication ESA-SP-1200
- Escorza, A., Boffin, H. M. J., Jorissen, A., et al. 2017, *A&A*, 608, A100
- Escorza, A., Karinkuzhi, D., Jorissen, A., et al. 2019a, *A&A*, 626, A128
- Escorza, A., et al. 2019b, this conference
- Gaia* Collaboration, Babusiaux, C., van Leeuwen, F., et al. 2018, *A&A*, 616, A10
- Giuricin, G., Mardirossian, F., & Mezzetti, M. 1983, *ApJS*, 52, 35
- Gontcharov, G. A. 2012, *Astronomy Letters*, 38, 87
- Gosnell, N. M., Mathieu, R. D., Geller, A. M., et al. 2014, *ApJ*, 783, L8
- Gosnell, N. M., Mathieu, R. D., Geller, A. M., et al. 2015, *ApJ*, 814, 163
- Green, P. J., Montez, R., Mazzoni, F., et al. 2019, *ApJ*, in press [arXiv:1905.07045](https://arxiv.org/abs/1905.07045)
- Gustafsson, B., Edvardsson, B., Eriksson, K., et al. 2008, *A&A*, 486, 951
- Hansen, T. T., Andersen, J., Nordström, B., et al. 2016, *A&A*, 588, A3
- Heber, U. 2016, *PASP*, 128, 082001
- Jancart, S., Jorissen, A., Babusiaux, C., et al. 2005, *A&A*, 442, 365
- Jones, D., & Boffin, H. M. J. 2017, *Nature Astronomy*, 1, 0117
- Jones, D., Van Winckel, H., Aller, A., et al. 2017, *A&A*, 600, L9
- Jorissen, A., Van Eck, S., Van Winckel, H., et al. 2016, *A&A*, 586, A158
- Jorissen, A., Boffin, H. M. J., Karinkuzhi, D., et al. 2019, *A&A*, 626, A127
- Kamath, D., Wood, P. R., & Van Winckel, H. 2014, *MNRAS*, 439, 2211
- Kamath, D., Wood, P. R., & Van Winckel, H. 2015, *MNRAS*, 454, 1468
- Kamath, D., Wood, P. R., Van Winckel, H., et al. 2016, *A&A*, 586, L5
- Käppeler, F., Gallino, R., Bisterzo, S., et al. 2011, *Reviews of Modern Physics*, 83, 157
- Karakas, A. I., & Lugaro, M. 2016, *ApJ*, 825, 26
- Lindgren, L. 2018, *Gaia-C3-TN-LU-LL-124-01* technical note, available at http://www.rssd.esa.int/doc_fetch.php?id=3757412
- Luri, X., Brown, A. G. A., Sarro, L. M., et al. 2018, *A&A*, 616, A9
- Manick, R., Kamath, D., Van Winckel, H., et al. 2019, *A&A*, in press ([arXiv:1906.10492](https://arxiv.org/abs/1906.10492))
- Massevitch, A., & Yungelson, L. 1975, *MmSAI*, 46, 217
- Mayer, A., Deschamps, R., & Jorissen, A. 2016, *A&A*, 587, A30
- McClure, R. D., & Woodsworth, A. W. 1990, *ApJ*, 352, 709
- McClure, R. D. 1997, *PASP*, 109, 536
- McCrea, W. H. 1964, *MNRAS*, 128, 147
- Merle, T., Jorissen, A., Masseron, T., et al. 2014, *A&A*, 567, A30
- Merle, T., Jorissen, A., Van Eck, S., et al. 2016, *A&A*, 586, A151
- Mermilliod, J.-C., Andersen, J., Latham, D. W., et al. 2007, *A&A*, 473, 829
- Milliman, K. E., Mathieu, R. D., & Schuler, S. C. 2015, *AJ*, 150, 84
- Miszalski, B., Boffin, H. M. J., Frew, D. J., et al. 2012, *MNRAS*, 419, 39
- Miszalski, B., Boffin, H. M. J., Jones, D., et al. 2013a, *MNRAS*, 436, 3068
- Miszalski, B., Boffin, H. M. J., & Corradi, R. L. M. 2013b, *MNRAS*, 428, L39
- Mohamed, S., & Podsiadlowski, P. 2012, *Baltic Astronomy*, 21, 88

- Oomen, G.-M., Van Winckel, H., Pols, O., et al. 2018, *A&A*, 620, A85
- Paczyński, B. 1971, *ARA&A*, 9, 183
- Peters, G. J. 2001, in *The Influence of Binaries on Stellar Population Studies*, ed. Vanbeveren D. (Kluwer Academic Publishers, Dordrecht), *Astrophysics and Space Science Library*, 264, 79
- Pourbaix, D., & Jorissen, A. 2000, *A&AS*, 145, 161
- Pourbaix, D., Tokovinin, A. A., Batten, A. H., et al. 2004, *A&A*, 424, 727
- Pourbaix, D. 2019, this conference
- Preston, G. W., & Sneden, C. 2000, *AJ*, 120, 1014
- Refsdal, S., Roth, M. L., & Weigert, A. 1974, *A&A*, 36, 113
- Roulston, B. R., Green, P. J., Ruan, J. J., et al. 2019, *ApJ*, 877, 44
- Sana, H., de Mink, S. E., de Koter, A., et al. 2012, *Science*, 337, 444
- Sarna, M. J. 1993, *MNRAS*, 262, 534
- Siess, L., Davis, P. J., & Jorissen, A. 2014, *A&A*, 565, A57
- Sneden, C., Preston, G. W., & Cowan, J. J. 2003, *ApJ*, 592, 504
- Sperauskas, J., Zács, L., Schuster, W. J., et al. 2016, *ApJ*, 826, 85
- Subramaniam, A., Sindhu, N., Tandon, S. N., et al. 2016, *ApJ*, 833, L27
- Szabados, L. 2003, *Information Bulletin on Variable Stars*, 5394, 1
- Szabados, L. 2019, *Contributions of the Astronomical Observatory Skalnaté Pleso*, 49, 171
- Thevenin, F., & Jasiewicz, G. 1997, *A&A*, 320, 913
- Tout, C. A., & Eggleton, P. P. 1988, *MNRAS*, 231, 823
- Tyndall, A. A., Jones, D., Boffin, H. M. J., et al. 2013, *MNRAS*, 436, 2082
- Van der Swaelmen, M., Boffin, H. M. J., Jorissen, A., et al. 2017, *A&A*, 597, A68
- van Rensbergen, W., De Loore, C., & Jansen, K. 2006, *A&A*, 446, 1071
- van Rensbergen, W., de Greve, J. P., Mennekens, N., et al. 2011, *A&A*, 528, A16
- Van Winckel, H. 2003, *ARA&A*, 41, 391
- Van Winckel, H., Jorissen, A., Exter, K., et al. 2014, *A&A*, 563, L10
- Vos, J., Østensen, R. H., Degroote, P., et al. 2012, *A&A*, 548, A6
- Vos, J., Vučković, M., Chen, X., et al. 2019, *MNRAS*, 482, 4592
- Webbink, R. F. 1984, *ApJ*, 277, 355
- Webbink, R. F. 1985, in *Interacting Binary Stars*, eds. J.E. Pringle & R.A. Wade, (Cambridge University Press, Cambridge), 39
- Whitehouse, L. J., Farihi, J., Green, P. J., et al. 2018, *MNRAS*, 479, 3873
- Wright, E. L., Eisenhardt, P. R. M., Mainzer, A. K., et al. 2010, *AJ*, 140, 1868